Supplementary Information

Advanced 96-microtiter plate based bioelectrochemical platform reveals molecular short cut of electron flow in cytochrome P450 enzyme

Ronny Frank[a], Christoph Prönnecke [a], Ronny Azendorf[a], Heinz-Georg Jahnke[a], Annette G. Beck-Sickinger[b], Andrea A. Robitzki[a]*

Authors' Affiliations

[a]Centre for Biotechnology and Biomedicine, Molecular biological-biochemical Processing Technology, Leipzig University, Deutscher Platz 5, D-04103 Leipzig, Germany

[b]Institute of Biochemistry, Leipzig University, Brüderstraße 34, D-04103 Leipzig, Germany

* Corresponding author: E-mail: andrea.robitzki@bbz.uni-leipzig.de
Phone: +49 341 9731241
Fax: +49 341 9731249

Total Number of Figures and Tables: 15 Figures, 3 Tables

SUPPLEMENTARY MATERIALS AND METHODS

Cloning of P450 BM3 FT6H triple mutant and enzyme expression

The coding sequence of the His-tagged P450 BM3 triple mutant A75G/F87V/L188Q was cloned into the pRSF-1b plasmid backbone (Novagen, Germany) and extended on the C-terminus with a threefold repetition of the surface binding peptide sequence RTHRK using standard PCR procedure (see Tab. S2).

Batch expression of P450 BM3 was conducted in E.coli strain BL21 (DE3) (Life Technologies, Germany) using terrific broth (TB) media, which was produced according

to Cold Spring Harbor protocol and supplemented with 100 µg/L kanamycin (Carl-Roth, Germany), 0.1 mM δ-aminolevulinic acid hydrochloride (Sigma Aldrich, Germany), 30 µM $FeCl_2$; (Merck, Germany), 1.5 µM, riboflavin (Applichem, Germany) and 25 µM thiamine hydrochloride (Sigma Aldrich, Germany). Cells were grown to an OD of 0.6-0.8 at 37°C and 250 rpm (Noctua IH 50), before protein expression was initiated with 1 mM IPTG (Applichem, Germany) and temperature was reduced to 30°C and was hold for 20 h. Cells were harvested by centrifugation (Labofuge 400R, Heraeus, Germany) and pellets were stored at -80°C in 0.3 g aliquots until further use. Cells, in which protein expression was not induced by IPTG, were harvested after cultivation for 6 h at 30°C.

Addition of a surface binding motif to the C-terminus of P450 BM3 mutant A74G/L87V/L188Q led to enzyme variant FT6H:

C-Terminus	GHHHHHHGRTHRKRTHRKRTHRK
Primer	CGATCTCGAGTCACTTCCTATGCGTTCTCTTTCGGTGAGTGC-GTTTACGATGGGTACGTCCGTGATGGTGATGGTGGTGACCC

IMAC purification of cytochrome P450 BM3

E.coli BL21 cell pellets were resuspended in cold lysis buffer consisting of 40 mM Na_2HPO_4/NaH_2PO_4, 500 mM NaCl, 10 mM imidazole, 1 mg / 1 g pellet mass lysozyme, 3 mM magnesium chloride (Merck, Germany) and 10 µg/mL DNaseI (Applichem, Germany). Cells were disrupted by three runs in an ice-cooled french press (Thermo IEC, Germany) and lysate was incubated for 1.5 hours on ice. Cell fragments were separated by centrifugation (Hermle Z383K, Hereaus, Germany) at 8000 rpm for 20 minutes at 4°C and supernatant was transferred to a new vial. P450 BM3 was isolated by affinity chromatography performed with a His-Trap Crude FF 5 mL Column (GE Healthcare, Germany) on an ÄKTA Prime system (GE Healthcare, Germany). After loading, the

column was washed with binding buffer (40 mM Na_2HPO_4/NaH_2PO_4, 500 mM NaCl, 20 mM imidazole) and P450 BM3 was eluted with a linear imidazole gradient. Red-colored fractions containing BM3 were combined and immediately dialysed using Slide-A-Lyzer G2 Dialysis Cassettes with an exclusion limit of 10 kDa (Thermo Fisher, Germany) against phosphate buffered saline (PBS, pH 7.2) in the dark at 4°C. Purified P450 BM3 was aliquoted and stored at -80°C. Protein concentration was determined by Roti Nanoquant assay (Carl-Roth, Germany) and heme content assessed by CO-difference spectra analysis as described in previous studies (1).

Experimental procedure of the NADPH assay

NADPH assay of the immobilized enzyme was performed analogously to the bioelectrocatalytic procedure. Reaction solution contained additional 250 µM NADPH (Carl-Roth, Germany) and a NADPH regeneration system consisting of 50 mM glucose (Merck, Germany) and 1 U/mL glucose-dehydrogenase (Sigma Aldrich, Germany). The electrode main module was not used in this case.

NADPH assay of the enzyme in solution was performed in black 96 microtiter plates (Greiner). Reaction volume was 100 µL consisting of 50 nM enzyme, 250 µM NADPH, 50 mM glucose, 1 U/mL glucose-dehydrogenase and 1 mM 7-ethoxycoumarin. Reaction was stopped after 30 min using 100 µL of a 1.5 M glycine buffer (pH 10.2). In order to assess enzyme activity in solution without the regeneration system, NADPH concentration was raised to 500 µM and reaction time was reduced to 5 min.

References:

Determination of the sheet resistance of indium tin oxide

The resistance R was determined with a Voltcraft VC820 resistance measuring device on 20 mm long and 50 µm wide planar indium tin oxide electrodes with film thicknesses of

250 and 500 nm. From the resistance and the electrode geometry, we calculated the bulk resistivity ρ to be 1.14±0.05 x 10^{-3} Ωcm. Film thicknesses were determined by atomic force microscopy (AFM) using a JPK Nanowizard III (Bruker). Fig. S1 shows an example of an AFM measurement for the used multi electrode arrays with pear-shaped electrodes. Film thicknesses are typically in the range of 300-600 nm, corresponding to a sheet resistance range of 19-38 Ω/sq.

Bonding of the multi electrode array to the microtiter plate

The multi electrode array is bonded to the prepared microtiter plate using a mechanical press (Fig.S2). The developed device guarantees that the position of the microtiter plate precisely matches the position of the electrodes, while ensuring complete contact between microtiter plate and the glass substrate of the multi electrode array. The position matching is performed in dry condition, i.e. prior to epoxy resin coating. For this purpose we have built an adjustment aid which allows to shift the position of the microtiter plate relative to the multi-electrode array by 2-3 mm in lateral direction and to fix this shift. When the matching procedure was performed, the bottom side of the microtiter plate is coated with epoxy resin. This step is carried out by spreading epoxy resin (25 min maturing time for the used resin to ensure a suitable level of viscosity) as a thin layer on the paper side of a sheet of Parafilm. Afterward, the microtiter plate is dipped in the epoxy resin layer, checked for complete coating and placed on the multi electrode array in the mechanical press. Due to the pre-matching procedure no position correction is necessary. The level of contact pressure is adjusted manually depending on the viscosity and layer thickness.

Finite element method (FEM) simulation

COMSOL Multiphysics 5.3 (Comsol Multiphysics GmbH) was used to simulate the diffusion of potassium chloride from the top to the bottom chamber. A simplified model of

the two chamber system (top chamber 8 mm height, 3.5 mm radius; bottom chamber 2 mm height, 3.5 mm radius) with the agarose bridge (8 mm height, 2 mm radius) was generated with mesh size “superfine”. To simulate the diffusion the module “transport of diluted species” was used. Starting conditions were 10 mM / 150 mM KCl in the bottom chamber and 3 M / 1 M KCl in the top chamber. The diffusion coefficient of potassium chloride was set to $1.844 \cdot 109$ m^2/s (2). Based on the time-dependent simulation results, concentration values were extracted with a virtual probe positioned in the center, 0.1 mm above the bottom of the bottom chamber.

References

1. Omura T, Sato R. The carbon monoxide-binding pigment of liver microsomes: I evidence for its hemoprotein nature. J Biol Chem. 1964;239:2370-8.
2. He MG, Zhang S, Zhang Y, Peng SG. Development of measuring diffusion coefficients by digital holographic interferometry in transparent liquid mixtures. Opt Express. 2015;23(9):10884-99.
3. Frank R, Klenner M, Azendorf R, Bartz M, Jahnke H-G, Robitzki AA. Novel 96-well quantitative bioelectrocatalytic analysis platform reveals highly efficient direct electrode regeneration of cytochrome P450 BM3 on indium tin oxide. Biosens Bioelectron. 2017;93:322-9.
4. Zernia S, Frank R, Weiße RH-J, Jahnke H-G, Bellmann-Sickert K, Prager A, et al. Surface-Binding Peptide Facilitates Electricity-Driven NADPH-Free Cytochrome P450 Catalysis. ChemCatChem. 2018;10(3):525-30.

Supplementary Figures

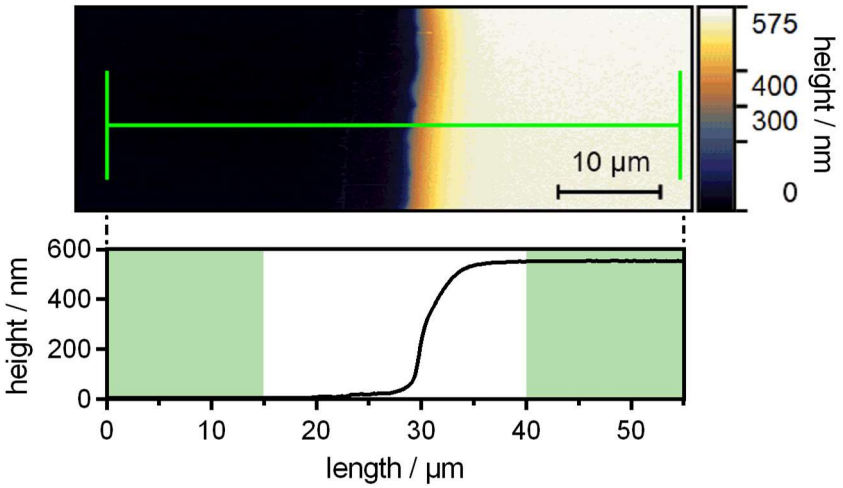

Fig.S1: Layer thickness of ITO electrode. Top: Example of contact-mode AFM measurement (cantilever DNP10, Bruker) to determine the thickness of the electrodes on a glass substrate. Height profiles were extracted using Gwyddion 2.47 after three-point based plane levelling. Green line marks the area for profile extraction. **Bottom:** Extracted height profile. Green area was used for height calculation.

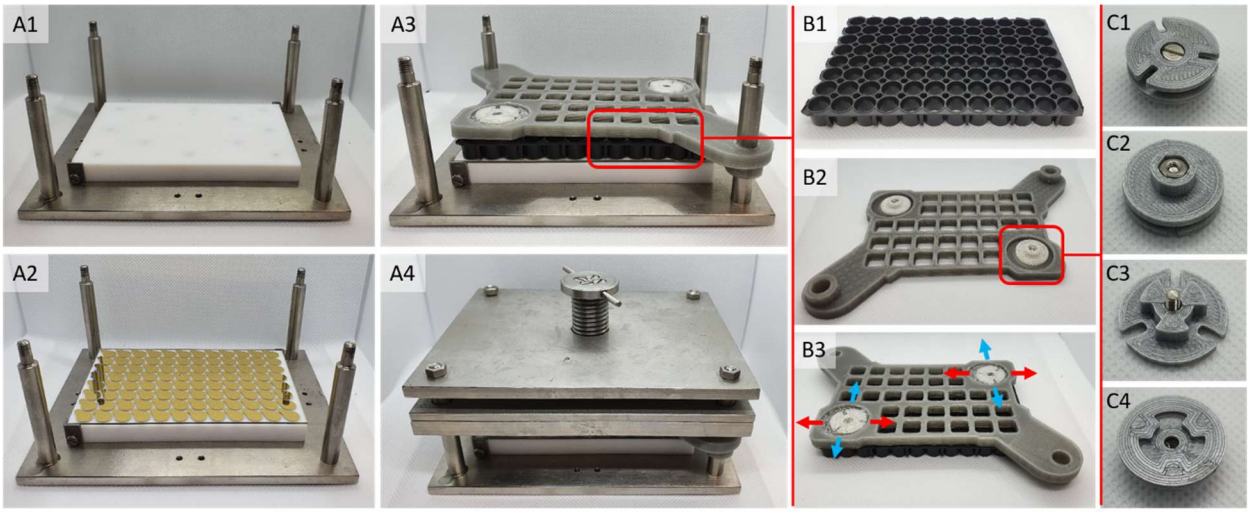

Fig.S2: Device for bonding multi electrode arrays to 96-well microtiter plates. A1 Base unit with PTFE block to lock off the multi electrode array. **A2** Base unit with multi electrode array in position (for better contrast in this picture, gold instead of ITO was used as electrode material). **A3** Microtiter plate precisely positioned with an adjusting aid to match the positions of the electrodes. **A4** Mechanical press. **B1** Microtiter plate **B2** Bottom side of the adjusting aid. **B3** Adjusting aid from top and clipped on the microtiter plate. Matching of the microtiter plate and the multi electrode array is performed before coating of the microtiter plate with epoxy resin. **C** Moveable element consisting of two parts, to change the position of the microtiter plate by 2-3 mm in lateral directions (**C1** Top side, **C2** Bottom side, **C3** Disassembled, bottom side of the upper part, **C4** Disassembled, top side of the lower part.)

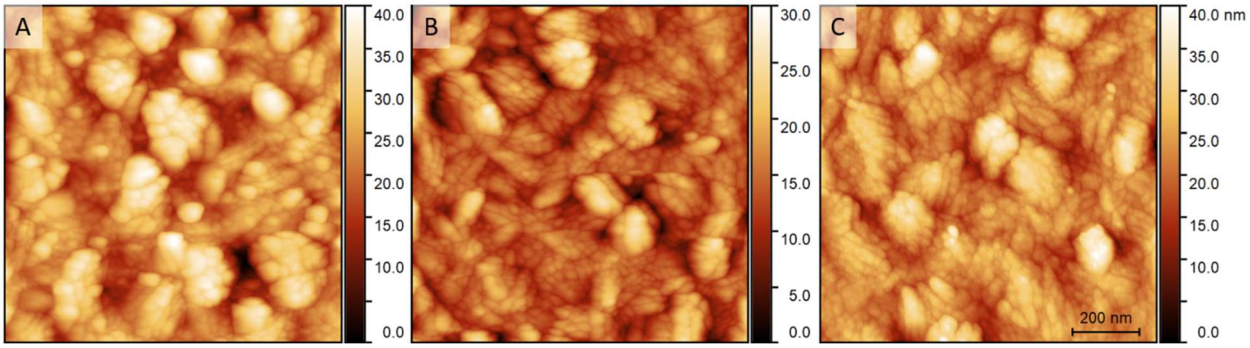

Fig.S3: Morphology of indium tin oxide dependent on cleaning step. Atomic force microscopy was performed in intermittent-contact mode using a TESP-HAR cantilever (Bruker) on a Nanowizard III (JPK Instruments, Bruker). **A** untreated electrode, **B** after modified RCA-1 treatment using a mix of H_2O_2(30%)/NH_3(25%)/H_2O (v/v/v, 1:1:5), **C** after 1N HCl treatment.

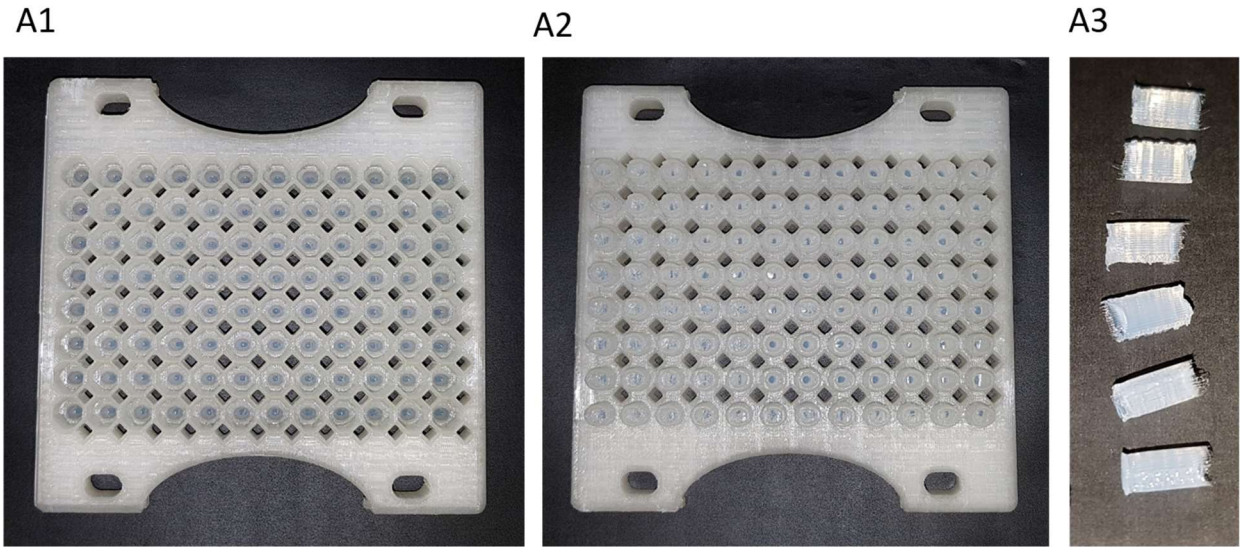

Fig.S4: Additional photographs of the 96-bioelectrocatalytic measurement platform. A1-A2 Top chamber module filled with agarose. **A3** Exemplary agarose bridges after ejection from the top chamber module. The ripped surface is visible, which is the result of the additive manufacturing process, and increases the surface area.

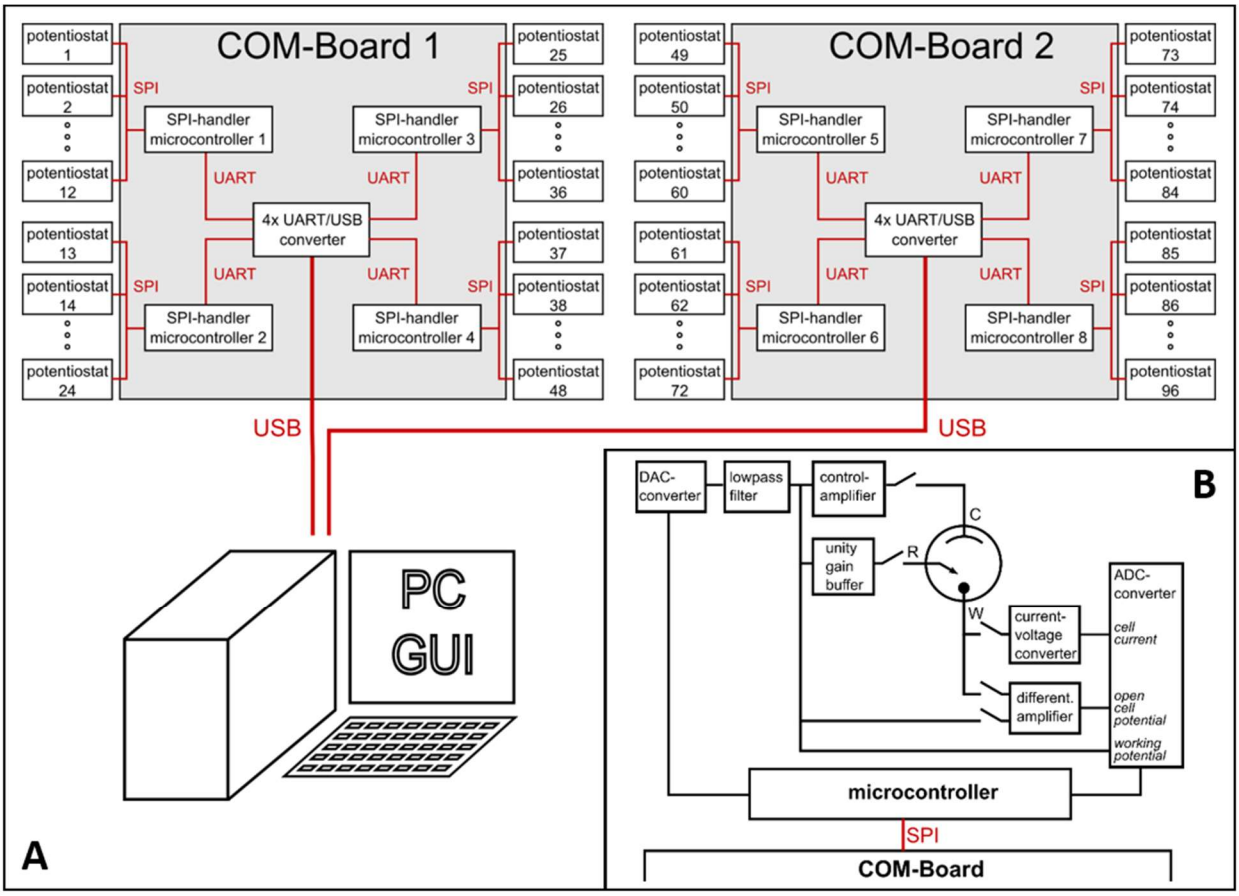

Fig.S5: Architecture of the 96-multipotentiostat and a single potentiostat module. A 96-multipotentiostat. **B** Simplified circuit of a single potentiostat module of microcontroller (ATXMEGA256), DA-converter (DAC8820) and AD-Converter (AD7367). Low-pass filter, control-amplifier, unity gain buffer, current-voltage converter and differential amplifier consists of an operational amplifier circuit (OPA277). The unity gain buffer acts as an operational amplifier to avoid current flow through the reference electrode.

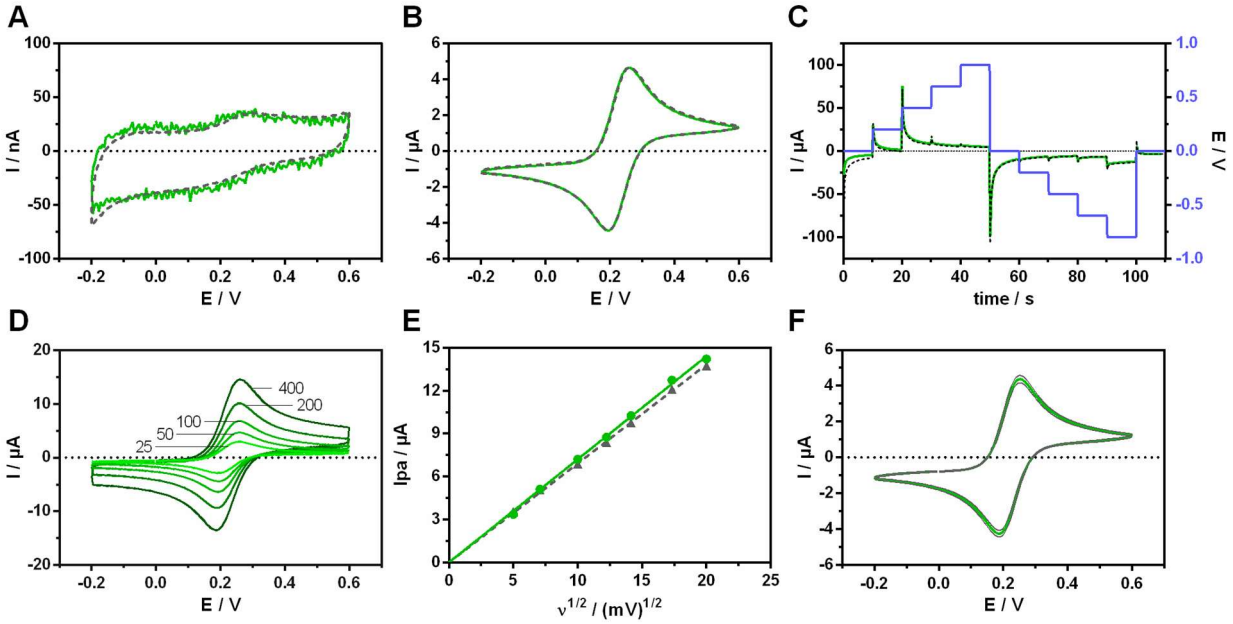

Fig.S6: Comparative measurements of the developed potentiostat modules and the IVIUM CompactStat potentiostat. Measurements took place in the bioelectrocatalytical system. 3-electrode setup for the CompactStat was established by using alligator clips connected to the

platin wire, the silver wire and the spring-loaded probe. Green Line: Developed potentiostat module, dashed line: CompactStat. **A** Low-current measurement using cyclic voltammetry with 0.5 M KCl and a scan rate of 25 mV/s. **B** Cyclic voltammogram of 0.2 mM ferri-/ferrocyanide in 0.5 M KCl at a scan rate of 50 mV/s, current values are in the typical range for a bioelectrocatalytic assay. **C** Constant potential measurement of 1 mM ferri-/ferrocyanide in 0.5 M KCl with potential steps after every 10 s. **D** Cyclic voltammograms of 0.1 mM ferri-/ferrocyanide in 0.5 M KCl for different scan rates from 25-400 mV/s. **E** Anodic peak potential from data shown in D, against the square root of the scan rate. **F** Mean cyclic voltammogram of all potentiostat modules of COM-board 1, showing standard deviation as black line. Working solution is the same as in B.

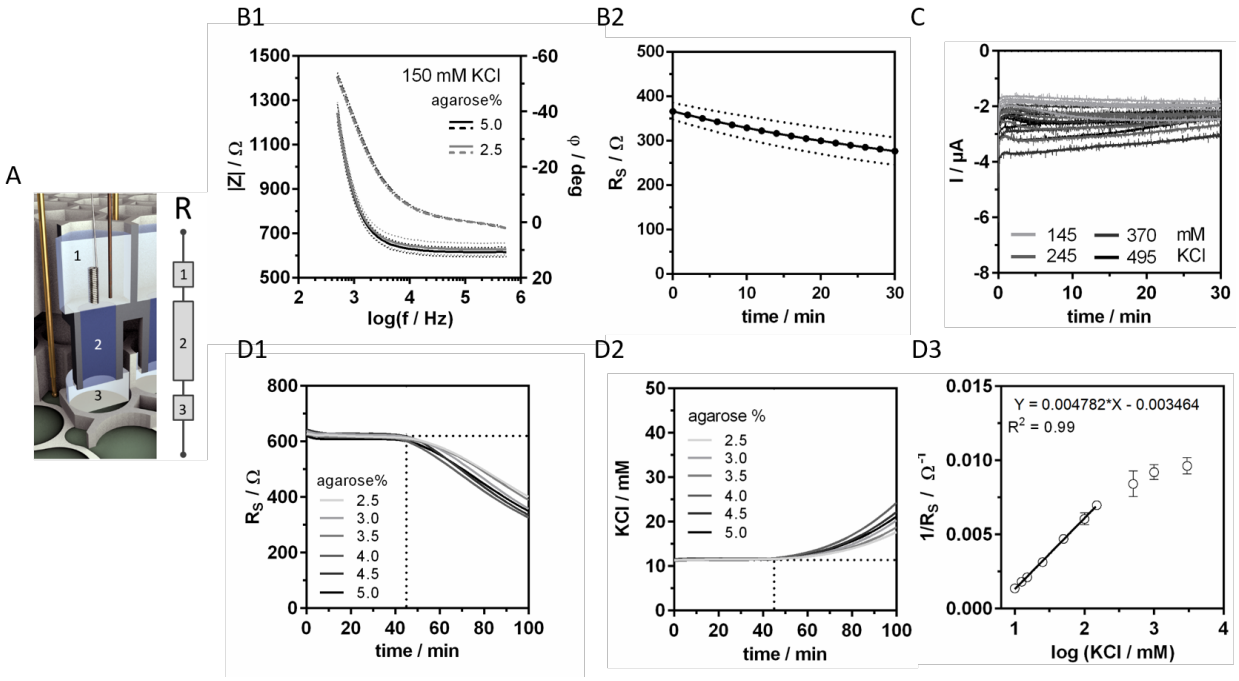

Fig.S7: Impedance analysis of the solution resistance in the bioelectrocatalytic 96-workstation. A Scheme of chamber-setup. Top chamber (1) with counter (platinum coil) and reference (Ag/AgCl rod) electrode, agarose bridge (2) and bottom chamber (3) with working electrode. **B1** Impedance measured between bottom and top chamber for a potassium chloride concentration of 150 mM, indicating that there is no influence of the agarose concentration on the determined spectra (solid line: magnitude, dashed line: phase). **B2** Decrease of the solution resistance between top and bottom chamber as a result of potassium and chloride ions migrating from high concentration in the top chamber (1 M KCl) into the agarose bridge (150 mM KCl). **C** Electrochemical data derived from the multipotentiostat during a bioelectrocatalytic measurement with different potassium chloride concentrations in the bottom chamber. **D1+D2** Stability of the reaction solution was assessed impedimetrically by measuring the solution resistance using an interdigital microelectrode structure in the bottom chamber at a starting potassium chloride concentration of 10 mM. Resistance drops, when potassium chloride of the top chamber (3 M) enters the bottom chamber. **D3** Calibration data to convert solution resistance to a potassium chloride concentration.

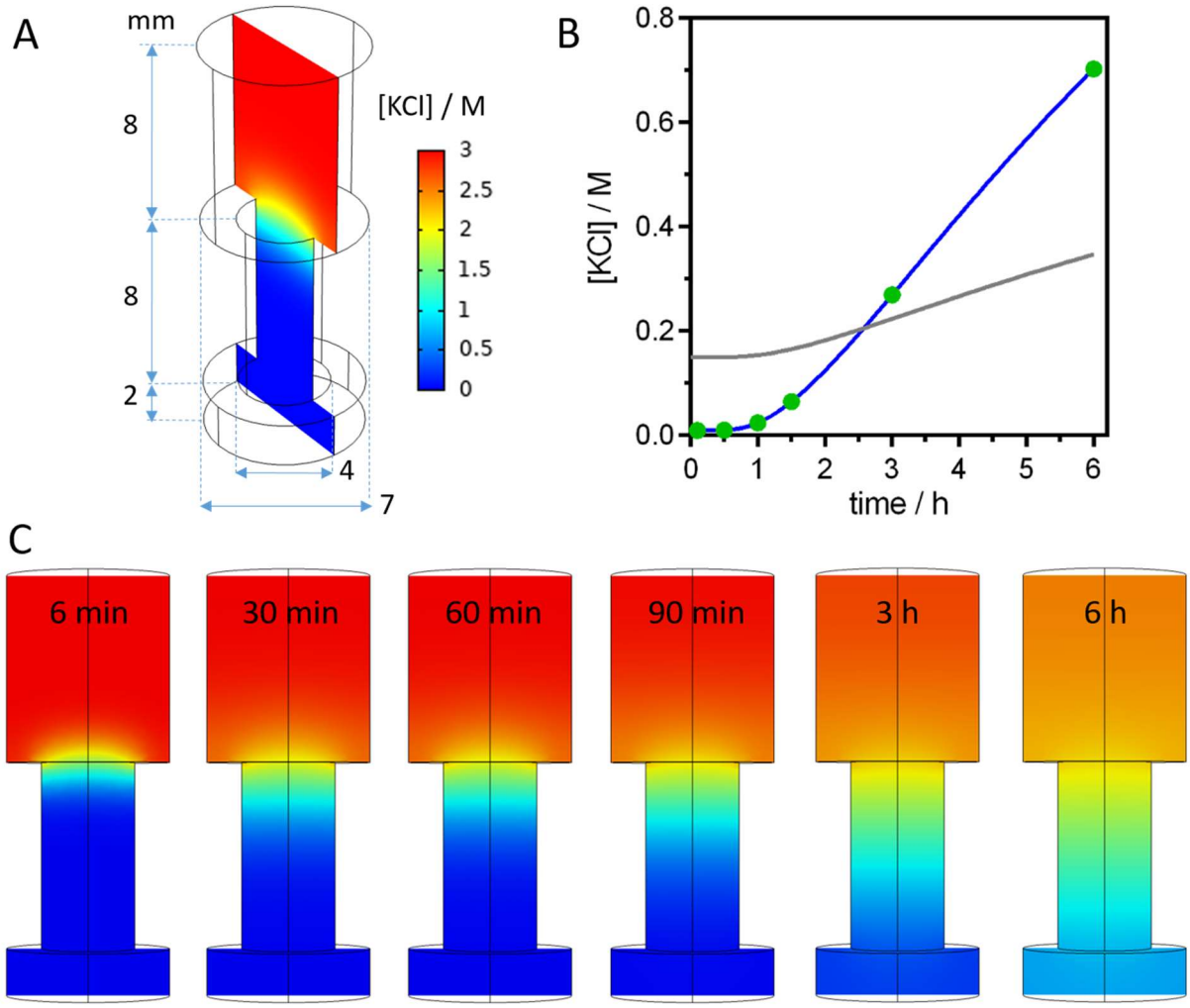

Fig.S8: FEM-Simulation of potassium chloride crossing from the top to the bottom chamber. A Simplified model of the vertical setup to simulate electrolyte crossing as performed in Fig.S2C. **B** Time-dependent change in potassium chloride in the bottom chamber when initially 10 mM KCl are present in the bottom chamber and 3 M in the top chamber (blue line), or when initially 150 mM KCl are present in the bottom chamber and 1 M in the top chamber (grey line). The blue line reaches 14 mM after 45 min and 65 mM after 90 min. **C** Distribution of potassium chloride for specific points in time (corresponding to the green dots from B).

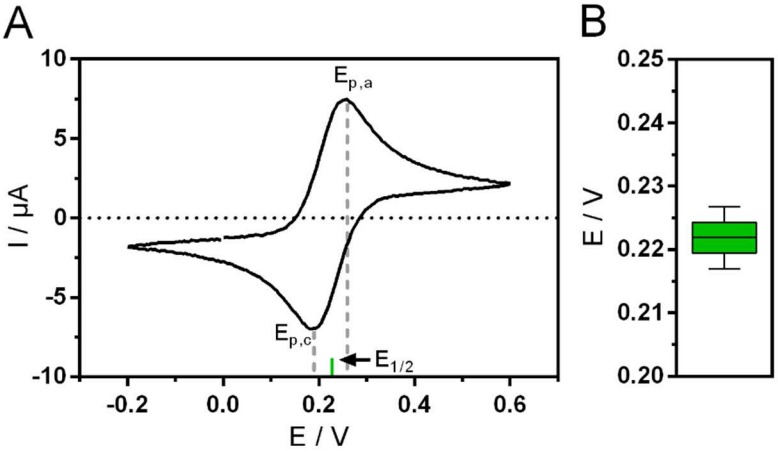

Fig.S9: Homogeneity of the half wave potential in the 96-measurement platform. A Representative example of a cyclic voltammogram when a solution of 0.2 mM ferri-/ferro cyanide in 0.5 M KCl is used in the bottom chamber with ITO working electrodes and a 1 M KCl solution

is in the top chamber where the Ag/AgCl reference electrode is located. Half wave potential is derived from the cathodic and anodic peak potential by the formula $E_{1/2} = 0.5 (E_{p,c} + E_{p,a})$. **B** Box plot with 25th and 75th percentile of the half wave potential of all 96 wells. Mean of the box plot is at 0.222 V with 25th percentile at 0.219 V and 75th percentile at 0.224 V, while the minimum value is 0.217 V and the maximum value is 0.227 mV. (n = 96) Although we do not measure the reference potentials of the Ag/AgCl electrodes itself (e.g. against NHE), we use the variance of the determined half wave potential of ferri/ferrocyanide as a measure of the variance of the Ag/AgCl electrodes.

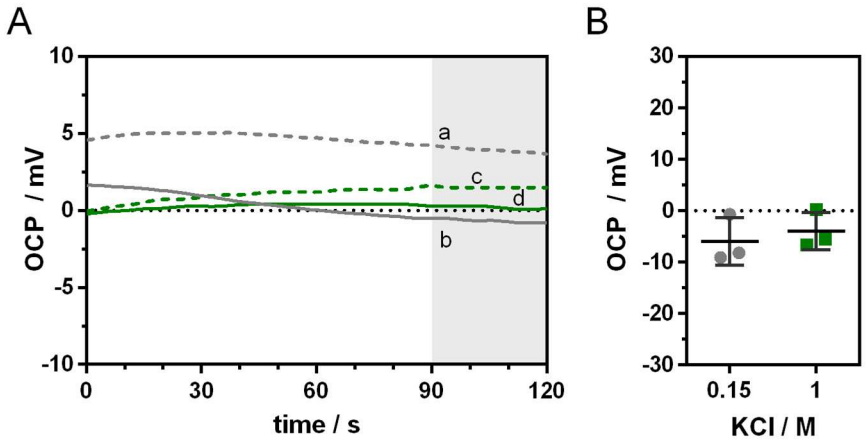

Fig.S10: Open cell potential measurement between the top and bottom chamber. A Example of the OCP measured between two platinum electrodes using the IVIUM CompactStat potentiostat. The potassium chloride concentration in bottom and top chamber and the agarose bridge was 150 mM. OCP was measured twice with a 30 s pause interval (a+b). Afterwards the electrolyte in the top chamber was replaced with 1 M KCl and OCP was measured again (c+d). **B** Three independent measurements of the OCP. Difference between the mean values is 2 mV. Values derived from the last 30 s of the b and d measurement (grey area in A).

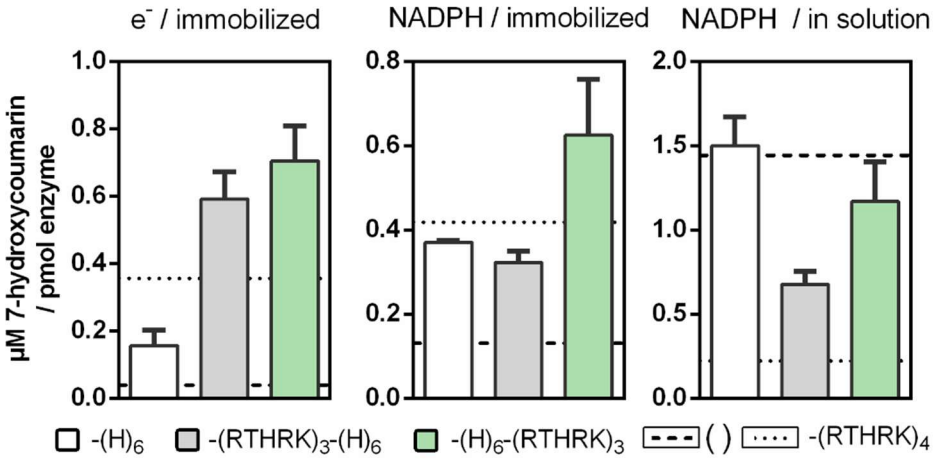

Fig.S11: Activity of N-terminally FLAG-tagged cytochrome P450 BM3 mutant A74G/ F87V/L188Q/ dependent on C-terminus. Activity was determined using the previously published method (3). Enzyme variants were tested bioelectrocatalytically and with NADPH after immobilisation as well as in solution. Tested BM3 variants with a C-terminal His-tag $(H)_6$ and/or surface-binding taq $(RTHRK)_n$ are shown in comparison with the variants without C-terminal tag (dashed line) or with solely the surface-binding tag (dotted line) from our previous publication (4).

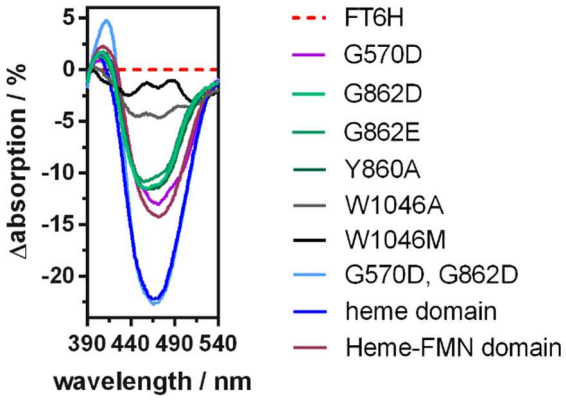

Fig.S12: Extended Dataset of UV/VIS difference spectra. Extended dataset of Fig.4B showing additional difference spectra of G862E, Y860A and the truncated variant without FAD-binding domain (Heme-FMN domain).

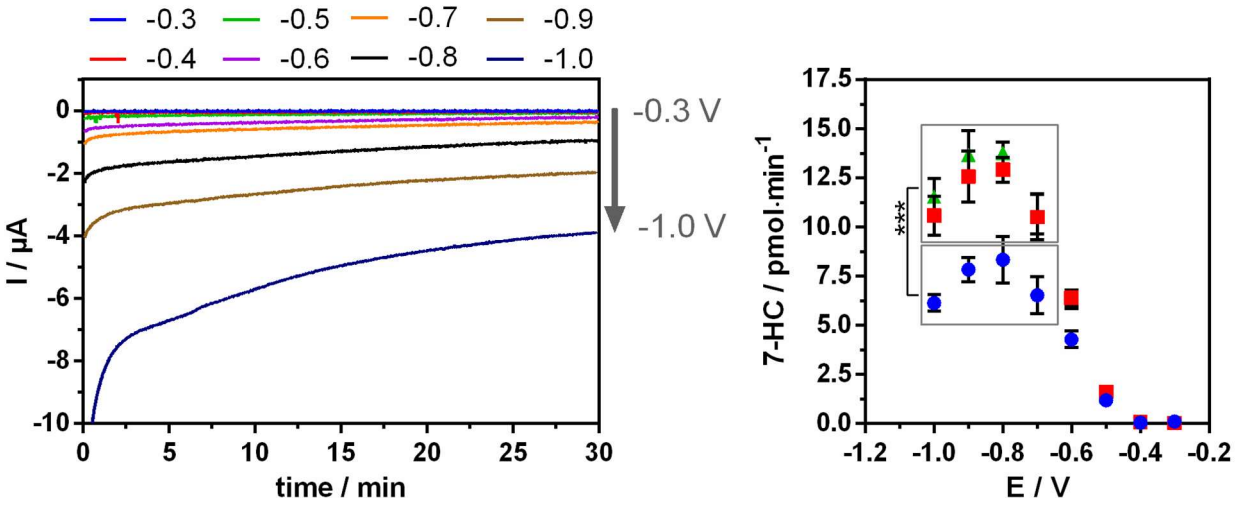

Fig.S13: Measurements of a constant potential series to evaluate the onset of enzyme activity of FAD- and FAD-deficient mutants. LEFT Electrochemical data during the constant potential series. RIGHT Bioelectrocatalytic activity of initial mutant FT6H (blue circles), mutant G862D (red squares) and Y860A (green triangles). (Mean+SEM, n=3, *** p = 0.001).

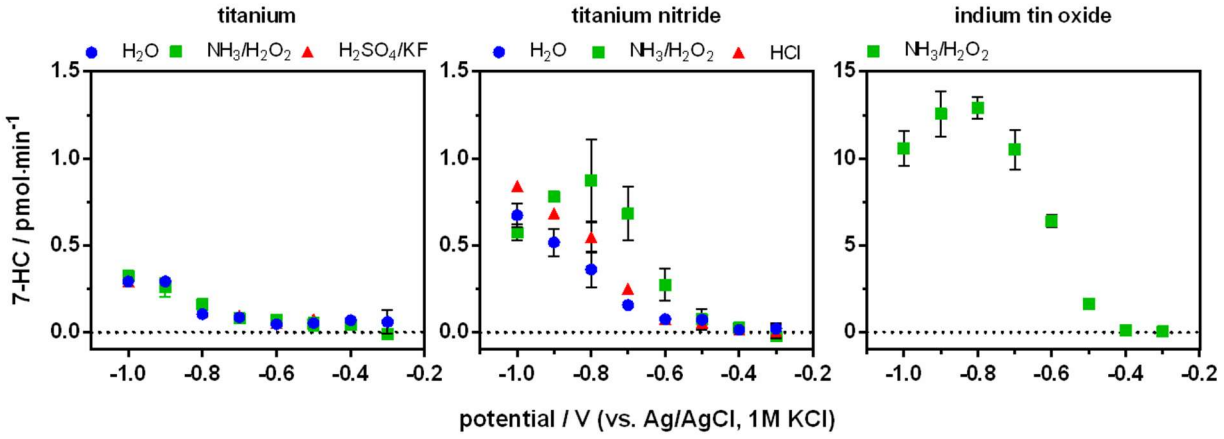

Fig.S14: Bioelectrocatalytic activity of Cytochrome P450 BM3 dependent on electrode material. LEFT Titanium electrodes were used without pretreatment (circles) or after 15 min in RCA-1 solution (H_2O_2(30%)/NH_3(25%)/H_2O (v/v/v, 1:1:5) or 2 min in 0.5 M H_2SO_4 + 5 mM KF (triangles). MIDDLE Titanium nitride electrodes were used without pretreatment (circles) or after 15

min in RCA-1 solution (squares) or after 10 min in 1N HCl (triangles). RIGHT Indium tin oxide electrode were used with the pretreatment procedure as described in the methods path. Bioelectrocatalytic activity was determined with the FT6H G862D mutant.

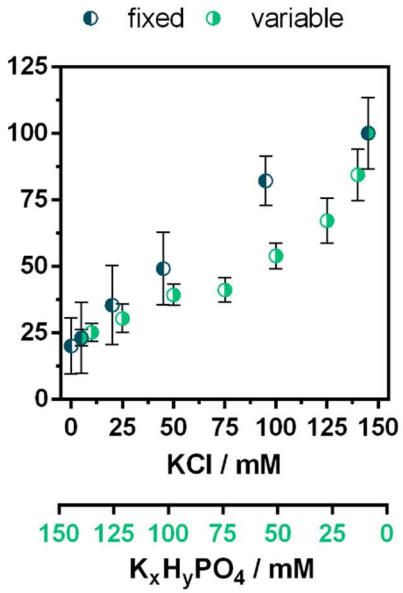

Fig.S15: Activity of P450 BM3 FT6H in solution in dependence of buffer composition. Comparison of the bioelectrocatalytic activity with a fixed hydrogenphosphate concentration of 5 mM and the variable ratio of chloride to hydrogenphosphate.

Supplementary Tables

Tab.S1: Solution resistance in the vertical three-electrode setup. Total solution resistance (R, Ω) measured by impedance spectroscopy between working and counter electrode in a one-chamber setup (i) or in the vertical two-chamber setup (ii) for different potassium chloride concentrations (M) in (**1**) the top chamber, (**2a**) the agarose bridge and (**3**) the bottom chamber. (2b) Agarose concentration of the electrolyte bridge (%).

	i	ii			
1	-	1.0	1.0	0.15	0.15
2a	-	0.5	0.15	0.15	0.15
2b	-	2.5	2.5	2.5	5.0
3	0.15	0.15	0.15	0.15	0.15
R	51±9	175±8	348±32	587±9	583±18

Tab.S2: N- and C-terminus of tested P450 BM3 triple mutant A74G/F87V/L188Q

Variant	N-Terminus	C-Terminus		
		tag 1	spacer	tag 2
FT	DYKDDDDK (FLAG-tag)	-	-	-
FTH		$(RTHRK)_4$	-	-
FT6		$(H)_6$	-	-
FTH6		$(H)_6$	G	$(RTHRK)_3$
FT6H		$(RTHRK)_3$	G	$(H)_6$

Tab.S3: Heme content of tested cytochrome P450 BM3 variants in raw cell extracts. Concentration was determined by CO Assay and is stated in µM.

	Not induced FT6H		Induced FT6H		Induced FT6		Purified FT6H	
Stock %	mean	SEM	mean	SEM	mean	SEM	mean	SEM
0.3	0.007	0.001	0.183	0.021	0.203	0.004		
0.5	0.011	0.001	0.275	0.031	0.304	0.007		
1.0	0.022	0.002	0.549	0.062	0.608	0.013		
2.0	0.044	0.004	1.099	0.125	1.216	0.027		
100	2.271	0.093	53.85	2.525	59.63	1.082	51.84	2.273